

# Influence of temperature on the mechanical behaviour of polyester fibres

C. Le Clerc · A. R. Bunsell · A. Piant

Received: 20 September 2005 / Accepted: 4 November 2005 / Published online: 20 September 2006  
© Springer Science+Business Media, LLC 2003

**Abstract** This study investigates the mechanical behaviour of polyester fibres over a range of temperatures by the use of a number of experimental techniques including tensile, creep and fatigue tests. The influence of temperature on the different mechanical properties is investigated with particular emphasis on the loss of rigidity and reduction of creep and fatigue lifetimes. A precise description of the stress/strain curves of the fibres highlights the effects with respect to the glass transition temperature. The fatigue failure process is precisely detailed and changes, at high temperature, to the classical fracture morphology observed are presented. A comparison between observations made of single fibres and yarns provides valuable information about the interpretation of results obtained with single fibre test to fibre assemblies.

## Introduction

Polyester drawn into fibres possesses very useful mechanical properties. The polyester used for fibres is polyethylene terephthalate (PET) and they are the most widely produced synthetic fibres. In addition to textile uses, they are widely used for technical products such as reinforcements in tyres or belting, geotextiles and mooring ropes. For all these different uses, the

mechanical loadings differ as well as the environmental and thermal conditions to which they are subjected.

PET fibres possess characteristics which are useful in technical applications: high tensile strength, low shrinkage, a good response to sustained loading, both in creep and fatigue. Temperatures encountered can vary from 4 °C on the ocean bed to more than 120 °C in tyre applications; some computer simulations predict an increase of temperature, from room temperature, to 100 °C for a biased truck tyre at 120 km/hr [1]. For the overall lifetime use of geotextiles, the alkalinity is of primary importance but temperature also accelerates degradation [2]. Furthermore, one of the experiments detailed below shows that the temperature of a simple yarn subjected, at ambient temperature, to oscillating mechanical stresses can reach 90 °C. Fibres can be in direct contact with air (cables) or water (ropes) or be enveloped in rubber or another polymer matrix. In each case, the thermal exchange rate differs so that the actual temperature of the fibres may be very different from the surrounding environment.

To describe the variation of mechanical behaviour of a thermoplastic with temperature, two different temperatures are important. First, the glass transition temperature ( $T_g$ ) separates a 'glassy' state from a highly deformable rubberlike state. The macroscopic mechanical properties are particularly dampened for amorphous materials: Initial modulus above  $T_g$  can be reduced to one tenth, or less, of its value below this temperature. In the glassy state, most of the molecular movements are frozen but the thermal energy provided by exceeding the glass transition temperature means that, greater molecular movement and new conformations become possible. Additional deformation is possible under load. The second important

---

C. Le Clerc (✉) · A. R. Bunsell · A. Piant  
Ecole des Mines de Paris, Centre des Matériaux, 91003 Evry  
Cedex, France  
e-mail: Christophe.leclerc@ensmp.fr

temperature is the melting point  $T_f$ , above which, no mechanical strength remains.

In order to describe the particularities of the semi crystalline structure of organic fibres, Prevorsek introduced the concept of microfibrils [3] and Oudet, macrofibrils [4], this model is presented on Fig. 1. A microfibril is a longitudinal succession of crystalline zones and intrafibrillar amorphous zones, with a width of the order of 5 nm. Oriented amorphous molecules occupy the spaces between fibrils and several fibrils make up a macrofibril and these are separated from others by an amorphous zone.

At room temperature, the fatigue failure of fibres shows a distinctive fracture morphology, very different from those obtained in creep or tensile tests. A crack is initiated at or just below the fibre surface, it grows longitudinally along the fibre axis, slightly penetrating into the fibre. The progressive reduction of the load bearing section leads to an increase of stress over the remaining section, and finally failure as in tensile or creep test. The final phase of failure shows an identical morphology to the tensile and creep cases with an initiation point, plastic deformation ahead of the crack and rapid failure normal to the fibre axis. This final tensile phase of fatigue failure is not initiated at the fatigue crack fracture surface but on or near the unbroken fibre surface.

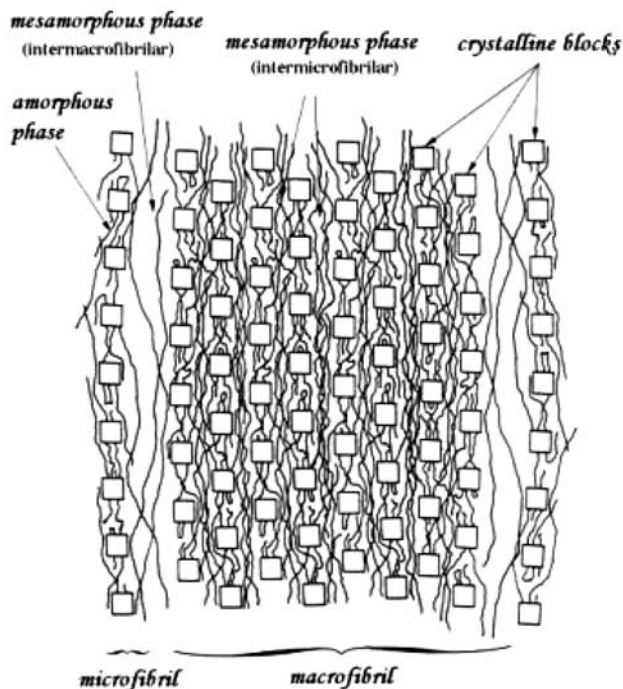


**Fig. 1** Oudet's model used to describe PET semicrystalline structure

Two complementary fracture surfaces are obtained, one showing a long tongue of material which can be seen to have been removed from the opposite complementary end as observed in many studies [4–9]. The length of the fatigue crack is often more than ten fibre diameters, and can be fifty times greater. Finally, the fatigue crack continues further than the final failure, as if the fatigue crack carries on progressing as creep damages the remaining load bearing section.

Given the wide uses to which PET are put and the wide range of conditions that they experience, it is necessary to determine precisely their mechanical properties over a wide range of temperatures. This study deals with this topic: it presents results concerning the mechanical behaviour of the PET fibres from room temperature to 180 °C, so encompassing the glass transition temperature. Tensile, creep and fatigue tests have been conducted; in order to avoid any ambiguities in interpreting the results, most tests were performed on single fibres which has required the use of testing equipment with great sensitivity for load and displacement measurements. The study has been completed with tests on yarns which will be shown to confirm and complement the results on single fibres and represent a step towards the understanding of the failure of tows used in structures.

## Experimental details

### Material

The polyester used for this study was a technical yarn with high modulus and low shrinkage (HMLS). Each fibre had a diameter of 18.5  $\mu\text{m}$  ( $\pm 0.8 \mu\text{m}$ ) and an initial modulus of 14 GPa ( $\pm 0.5 \text{ GPa}$ ), a tensile strength of 1 GPa ( $\pm 0.05 \text{ GPa}$ ) and elongation at tensile break of 12% ( $\pm 3\%$ ) at 20 °C. Fibres with these mechanical properties are obtained by high speed spinning so that the molecular orientation and the crystallinity are very high; the degree of crystallinity is about 50% and the birefringence is 0.221.

### Measurements on yarn

#### *Differential scanning calorimetry (DSC)*

The DSC studies were carried out in a nitrogen atmosphere, so as to avoid problems associated with oxidation, with a DSC 2920 modulated DSC from TA Instruments; the temperature range was 20–320 °C. The samples weighed 5–10 mg and were packed in

aluminium pans to ensure good heat diffusion. Two different DSC modes have been exploited. A classical DSC, with a heating rate of 10 °C/min, was used to study the melting characteristics. For the glass transition temperature, the modulated DSC was employed so that an oscillation of  $\pm 2$  °C each 80 s was superimposed on a heating rate of 5 °C/min. In this way, reversible and non reversible heat flows could be separated. The reversible heat flow permitted the glass transition temperature to be identified with accuracy.

#### *Dynamic thermomechanical analysis (DMTA)*

The thermomechanical studies have been carried out on a 01 dB Metravib machine (Viscoanalyser VA 4000); two different types of experiments have been conducted. First, classical DMTA studies were carried out on a yarn lightly loaded to around 1% of the tensile strength; a small oscillation extension at a fixed frequency while heating from 20 to 180 °C permitted the evolution of the modulus and the loss tangent with the temperature to be obtained. Several fixed oscillating frequencies were used in these tests, in the range from 5 to 100 Hz, so as to reveal the effect of time on the measured value of  $T_g$ .

The Multidyn software from Metravib allowed fatigue tests on entire yarns to be performed: for example 200,000 cycles of oscillation, from 0 to 70% of the tensile strength, at 50 Hz. A thermocouple was adapted to measure any increase in temperature. A difficulty was to find suitable clamps to hold the yarn; finally, smooth jaws and wrapping the yarn around a metal form positioned behind the grips avoided sliding and failure in the jaws.

#### Fibre testing machine

To test single fibres, Bunsell and Hearle developed an apparatus in the 1970s [10]. The fibre is held between two clamps, one connected to a piezoelectric sensor mounted on a screw thread connected to a motor controlling the crosshead, the other is fixed, for creep or tensile tests, or connected to a vibrator for fatigue tests. The key to this machine is the control of the load imposed on the fibre. A servomechanism compares the measured load to that required and if necessary, moves the cross-head so as to achieve the chosen load level. A tensile test consists of a controlled increase of load, at a constant chosen speed, until failure; a creep test consists however of an initial rapid load increase which then slows when within ten percent of the desired load so as to avoid overshooting. In a creep test, the load is

maintained constant until failure, with automatic compensation for the elongation which occurs during the test. Fatigue tests are similar to creep tests in that the loading conditions are maintained constant despite any elongation due to creep or plastic deformation, however a cyclic load is superimposed on a steady load. In a load controlled experiment, the maximum load is determined as the sum of the steady load and the amplitude (half crest to trough) of the cyclic load. This value is compared by the servo system to the required maximum load. A LVDT transducer monitors the displacement of the crosshead during a test. Fatigue tests can be chosen to be controlled either as a function of maximum load or displacement.

The main characteristics of this system are very precise load control, with an accuracy of 0.1 g between 0 and 100 g, a displacement with a precision of 1  $\mu\text{m}$  up to 20 mm. The vibrator is generally used at 50 Hz with a maximum displacement of  $\pm 3$  mm. In this study, the gauge length used was 30 or 50 mm, depending on the experimental conditions; in the case for which a large elongation was required a gauge length of 30 mm was used.

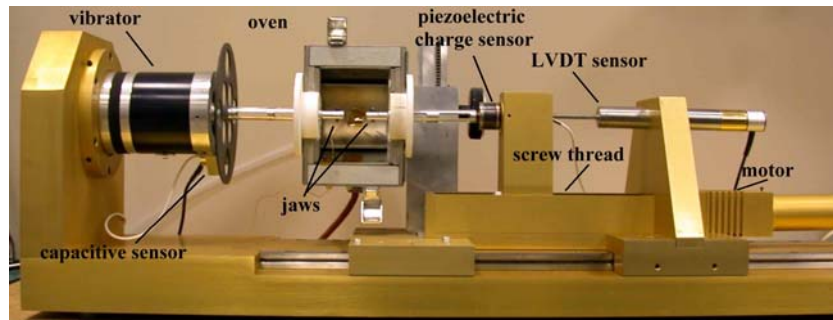
In order to investigate the behaviour of the fibres at temperature, a cylindrical heater was added to the machine; it enabled experiments from 20 °C to 300 °C to be carried out. The specimen was heated evenly over its whole length and the grips were introduced into the heating chamber. Hot jaws were chosen to avoid thermal gradients along fibre. An air cooling system was added to the grip linked to the piezoelectric transducer to avoid signal drift. Furthermore, to refine displacement data during fatigue test, a capacitive captor was added between the vibrator and grip. The testing apparatus is shown in Fig. 2.

The tensile tests were carried out with an elongation rate of 50%/min; so that, the whole test lasted about 20 s. More than 30 tests were performed at room temperature so as to determine the median properties of the fibres. At each other temperature at least four tests were carried out. The creep tests and fatigue tests were defined relative to a reference load which was the median breaking load of the fibre at the tested temperature and normalised to the fibre diameter. The stress/strain or strain/time curves were obtained using ATS software.

#### Scanning electron microscopy (SEM) observations

Fracture morphologies of broken fibres were observed with a Zeiss scanning electron microscope (Gemini 982). This microscope was equipped with a field effect gun which allowed working at low electron beam

**Fig. 2** Testing machine for single fibre, initially developed by Bunsell [5], with new adjunctions: oven and capacitive sensor



voltages which, in this study, were usually 2 kV. This ensured that the specimens were not damaged by the electron beam and gave improved images of the fibre surfaces. The fibres were coated with a 3 nm layer of gold/palladium to avoid charging problems.

## Results

### Tensile tests

The stress/strain curve of a polyester fibre presents a point of inflexion and a bending point which define three different regions; the effects of temperature on these regions are shown in Fig. 3. The first, from 0 to 2% strain, at room temperature, is elastic; the initial increasing gradient gives the initial modulus of the fibre. As the temperature was increased, this modulus was observed to fall: from 14 GPa at room temperature to 1.5 GPa at 180 °C (cf. Fig. 4). The decrease was not linear and an inflexion point can be seen to have occurred around 100 °C. The second region, between 2 and 9% strain, at room temperature, consisted of an almost straight line, the slope of which gave the second

modulus. The temperature was seen to have less influence on the second modulus, as it decreased only from 10.3 GPa to 6 GPa. The third region showed a fall in the slope of the curve, tending towards a stress plateau. The consequence of this behaviour was that there was a wider percentage dispersion in failure strains, which was around  $12 \pm 0.9\%$  at room temperature than for the breaking load which was around  $1 \pm 0.018$  GPa. The value of the stress plateau decreased regularly with increasing temperature, from 1 GPa at 20 °C to 0.7 GPa at 180 °C, as presented in Fig. 5. Over this temperature range, failure strain increased from 14% to more than 40%. The tensile test at 180 °C, shown in Fig. 3, presents a clear increase in strain to failure, and the stress strain curve has a markedly different shape from that at room temperature. During creep and fatigue tests, these variations have been taken into account.

The fracture morphologies of fibres broken in tension have been observed by scanning electron microscopy. The fracture morphologies presented in Fig. 6 show a two phase propagation process: first, at low speed, associated with plastic deformation around an initiation point just under the surface, and then rapid

**Fig. 3** Tensile tests of single fibre at different temperatures from 20 °C till 180 °C

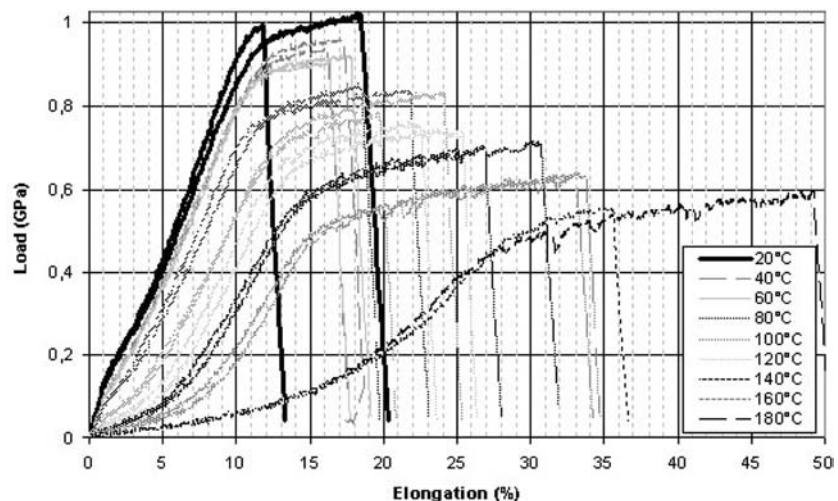


**Fig. 4** Initial modulus at different temperatures

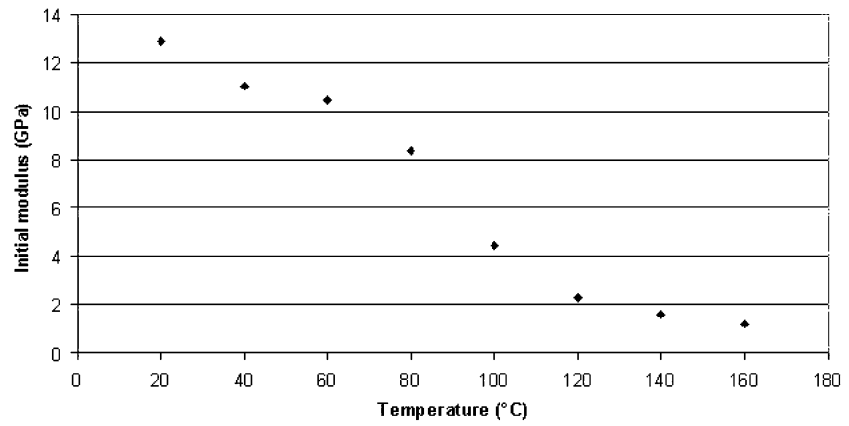


**Fig. 5** Elongation and load at break for PET fibres, at different temperatures

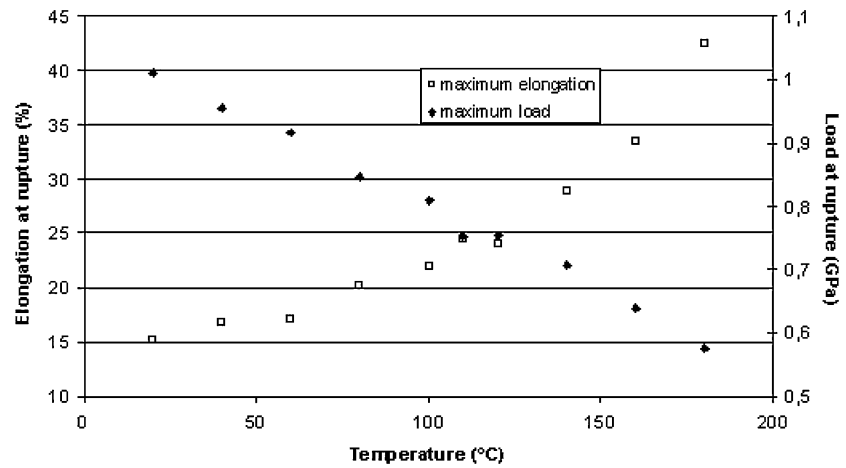
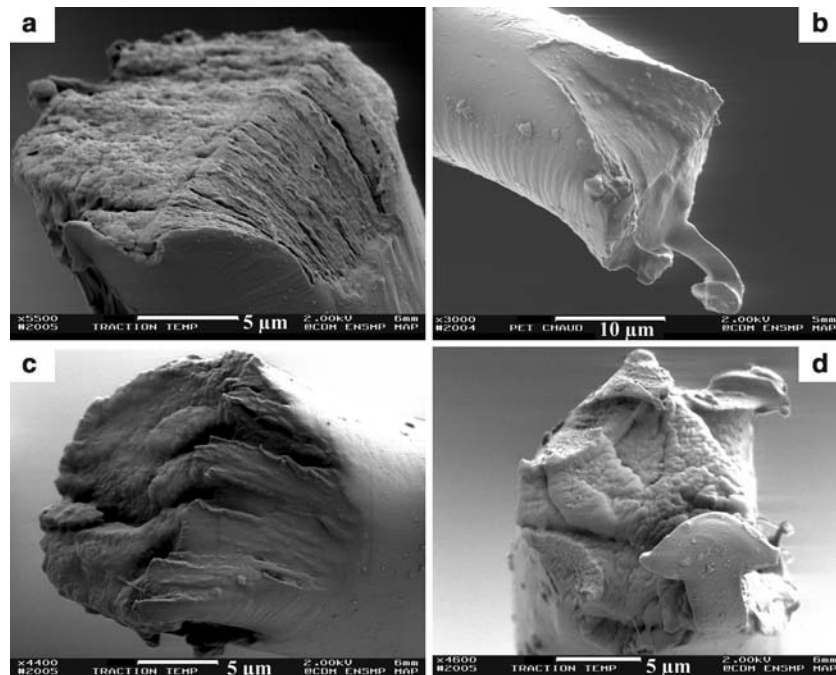


**Fig. 6** Fracture morphologies of tensile tests fibres, at 20 °C (a, b), 120°C (c), and 140 °C(d)



failure perpendicular to the fibre axis. The tensile failure is localised in the length of the fibre to less than the equivalent of the fibre diameter. Any effect of the temperature on the fracture morphology is not obvious, although, in a few cases, obtained at 80 °C or higher, crack initiation started at several separate points. At these higher temperatures the plastic deformation which occurred around the developing cracks was more complex than that seen at room temperature particularly around the initiation point leading to a less smooth bevelled region. The softening of the fibre which occurs above the  $T_g$  seems therefore to have some influence on the fracture morphology.

#### DMTA experiments

A typical result obtained with the DMTA at 50Hz, using a yarn specimen, is shown in Fig. 7; the modulus decreased during heating with an inflexion point around 120 °C. The loss tangent was calculated from the phase difference between the applied load and the induced strain over the whole temperature range studied. The glass transition temperature was taken as the maximum of the loss tangent which can be seen to have been around 136 °C for that yarn tested at 50 Hz. The shift between the curves obtained with an increasing temperature and the curves obtained with a decreasing temperature can be explained by a latent period corresponding to the time for all of the material to reach the oven temperature; however, for a lower rate of temperature increase, the difference between the values obtained for  $T_g$ , obtained with the two types of curve, decreased.

The  $T_g$  has been measured for different loading frequencies and the results are presented in Fig. 8. The glass transition temperature increased as the frequency increased as should be expected from the time temperature dependence relationship seen with

thermoplastics. Extrapolating the results with a zero heating rate, gave a value for the  $T_g$  of 127 °C from the loss tangent maximum; but for the point of inflexion in the Young modulus curve gives a value around 111 °C.

#### DSC experiments

In normal mode DSC, the heat flow revealed an endothermic peak centred at 257 °C, corresponding to polyester melting, the area under the peak allowed the percentage of crystallinity to be calculated, (Fig. 9). Thanks to the fusion enthalpy as  $DH_0 = 119\text{J/g}$ , the crystallinity percentage was found to be 48%, which is high for a semi crystalline polymer such as PET. The peak covered a range of temperatures but initiated around 200 °C. Modulated DSC experiments are presented in Fig. 10 and a slight inflexion point around 109 °C is noticeable during the reverse heat flow between 60 °C and 160 °C.

#### Creep tests on single fibres

Creep tests were carried out for different levels (80, 85 and 90%) of failure load at the different temperatures considered (20, 80, 120 °C). This means that, a test at 90% at 20 °C corresponded to 0.9 GPa, and at 120 °C, 0.7 GPa. For each thermal and mechanical condition, six or more tests have been conducted; their lifetimes at 20 °C are presented in Fig. 11. The median lifetime decreased with an increase in temperature or load, as shown in Fig. 12. There were more than three decades between the shortest time: 0.03 h at 90%, 80 °C and the longest 20 h at 70%, 20 °C. For identical imposed testing conditions, the median lifetime was divided by 3.5 from 20 °C to 80 °C and by further 2 from 80 °C to 120 °C. The fracture morphologies obtained were very similar to those obtained with

**Fig. 7** Typical DMTA results on a yarn at 50 Hz, 10 °C/min

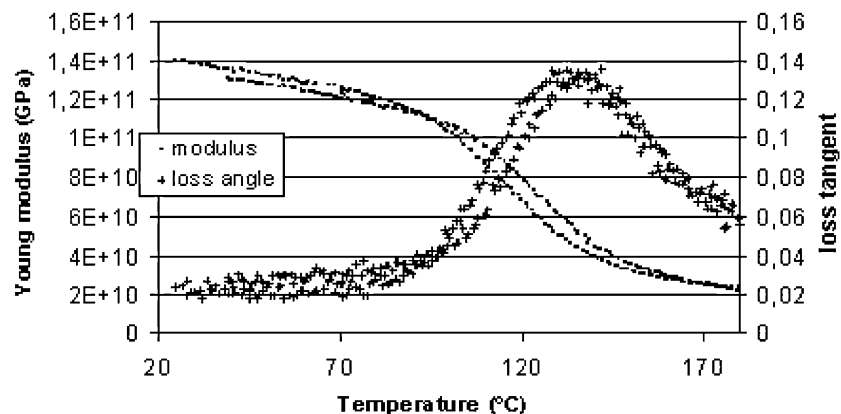


**Fig. 8** Glass temperature against frequency of oscillation with an heating rate of 10 °C/min

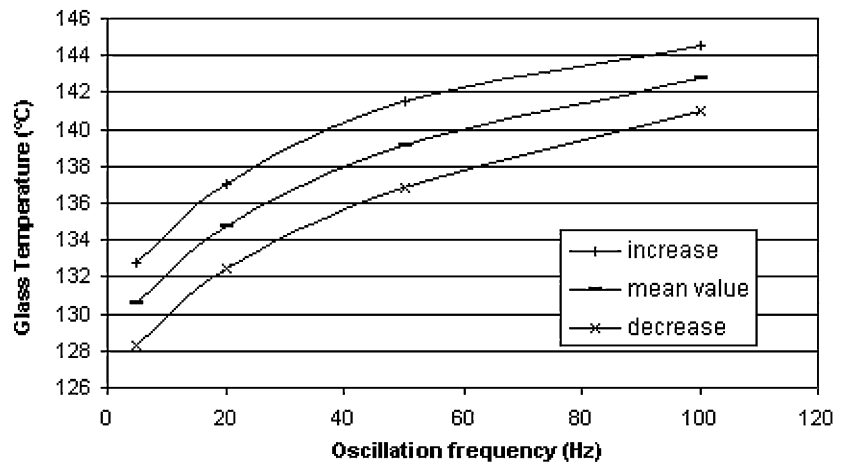


**Fig. 9** Classical DSC results on 5 mg of cutted fibres, peak of fusion centered at 257 °C

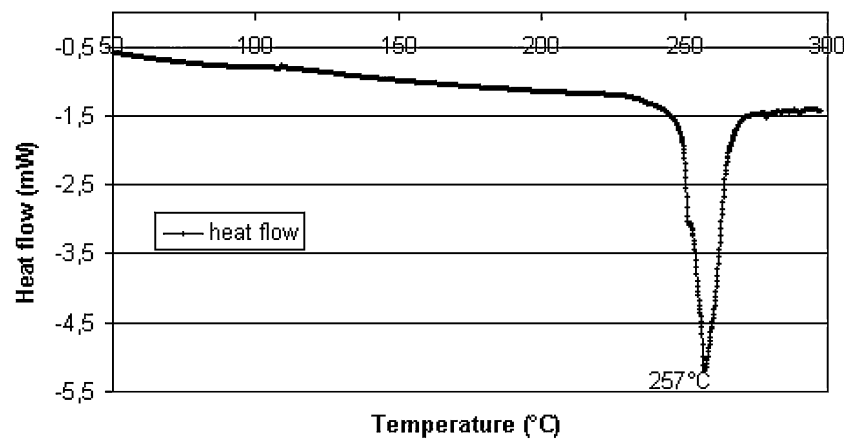
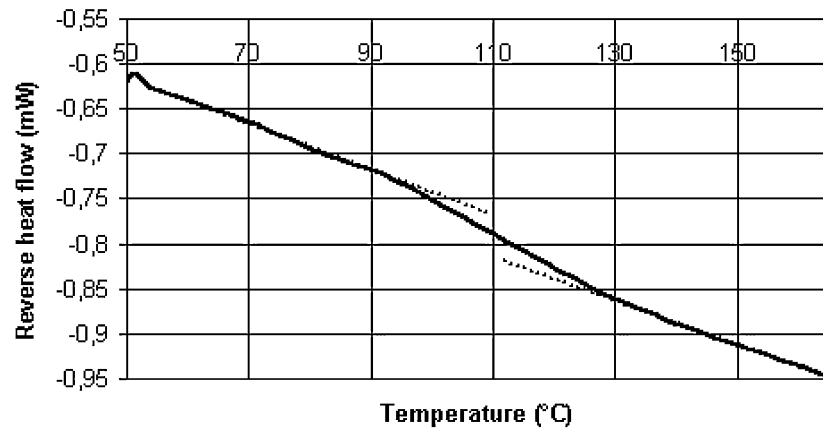


**Fig. 10** Modulated DSC on PET fibres, bending point centered around 110 °C



tensile tests showing initiation, subcritical propagation with plastic deformation and rapid failure. Examples are presented in Fig. 13. There are also similar variations, as seen in the tensile results, when tests results obtained at room temperature are compared to tests at higher temperatures with more initiation points appearing at 80 °C and 120 °C.

Fatigue tests on single fibres

In a similar way to that used for the creep tests, fatigue tests have been carried out for different mechanical and thermal conditions related to the simple tensile breaking loads for these conditions. Two mechanical parameters were controlled: the maximum load (70, 75

**Fig. 11** Lifetime of fibres submitted to creep test at 0.8, 0.85 and 0.9 Gpa at 20 °C i.e. 80%, 85% and 90% of the breaking load

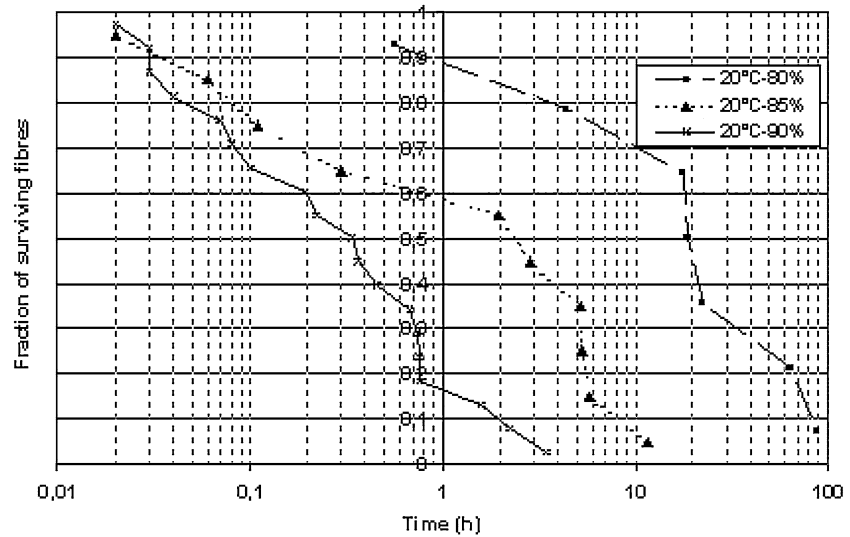


**Fig. 12** Median creep lifetimes for different conditions of temperature and load

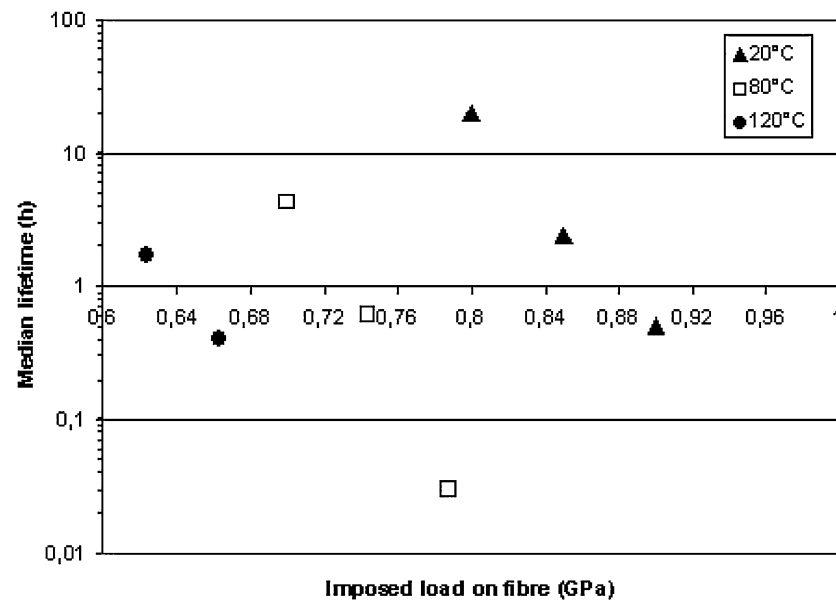
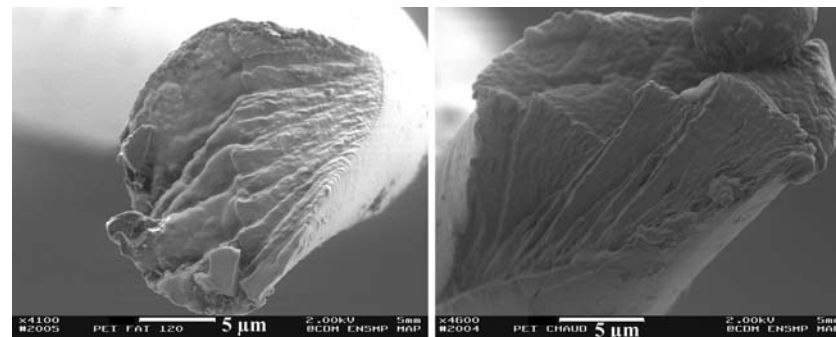


**Fig. 13** Fracture morphologies of fibres after creep tests at 20 °C and 120 °C



or 80%) and the minimum load (0, 5 or 10%), the influence of which is presented in Fig. 14. The influence of temperature was found to be similar to that for

creep tests: shorter lifetimes for hotter conditions, but the fall in lifetimes was less important: only being divided by 2 from 20 °C to 80 °C as presented in Fig. 15.



**Fig. 14** Influence of the maximum and minimum load on the fatigue test lifetime

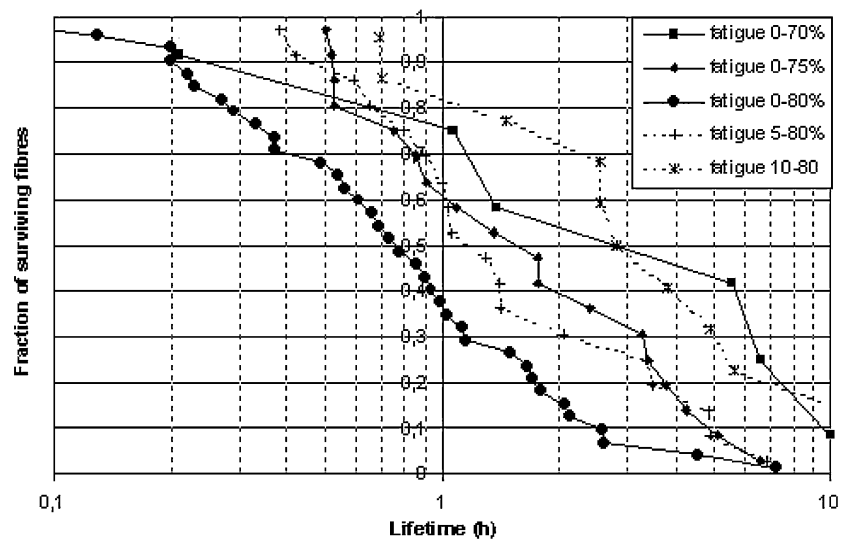
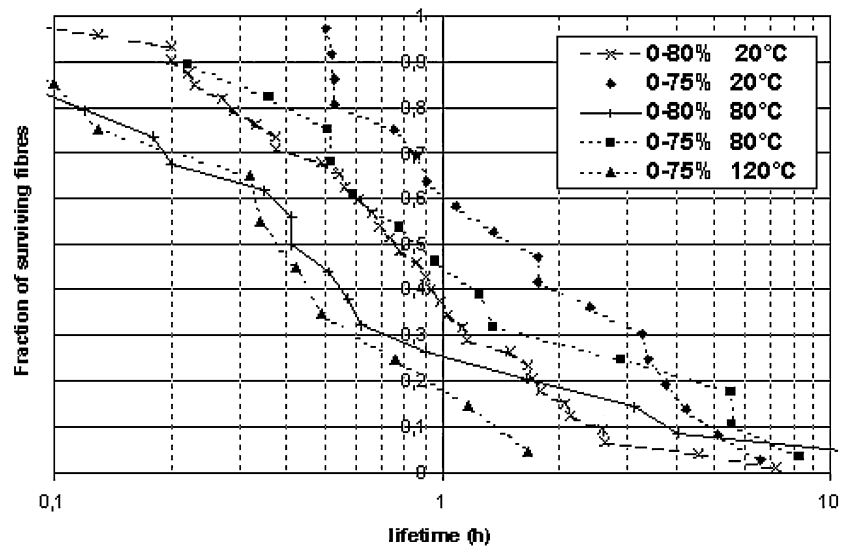


**Fig. 15** Influence of temperature on fatigue lifetimes, the tests are done relatively to tensile breaking load at the temperature of the test



The fracture morphologies of fibres subjected to fatigue conditions at room temperature presented classical specific complementary surfaces with a tongue on one part as can be seen in Fig. 16, it confirms what is found in the literature [4, 6–10].

Of the ten results observed at 80 °C, 3 fracture morphologies were identical to those observed at room temperature and seven showed very different morphologies with symmetrical breaks being observed, however not as in tensile or creep breaks. Both broken ends reveal, at least one longitudinal crack of 2 to 10 fibre diameters length, which have been termed truncated tongues. Around each truncated tongue and near the final failure, there is a deformed zone of similar size as the plastic deformation zone observed in creep or tensile breaks. However the zone presents a number of

sharp angles and bevelled terminations. The fatigue failure of fibres at 120°C all showed a truncated tongue as shown in Fig. 17.

#### Fatigue tests on yarns

A yarn of around 400 parallel fibres was found to have a tensile failure load of 9.8N; fatigue tests were carried out using the DMTA machine at room temperature. As with the single fibre tests, the minimum and maximum loads used have been expressed relative to breaking loads at the test temperature. Several yarn specimens were subjected to 100,000 or 200,000 cycles from 0% or 5% to 65% or 70% of breaking load without complete yarn failure. In these specimens, only some of the fibres were observed to

**Fig. 16** Fracture morphologies of fibres after fatigue test (0–80% during 0.78 h), the two parts are complementary, third picture: details of final failure (0–80% during 0.86 h)

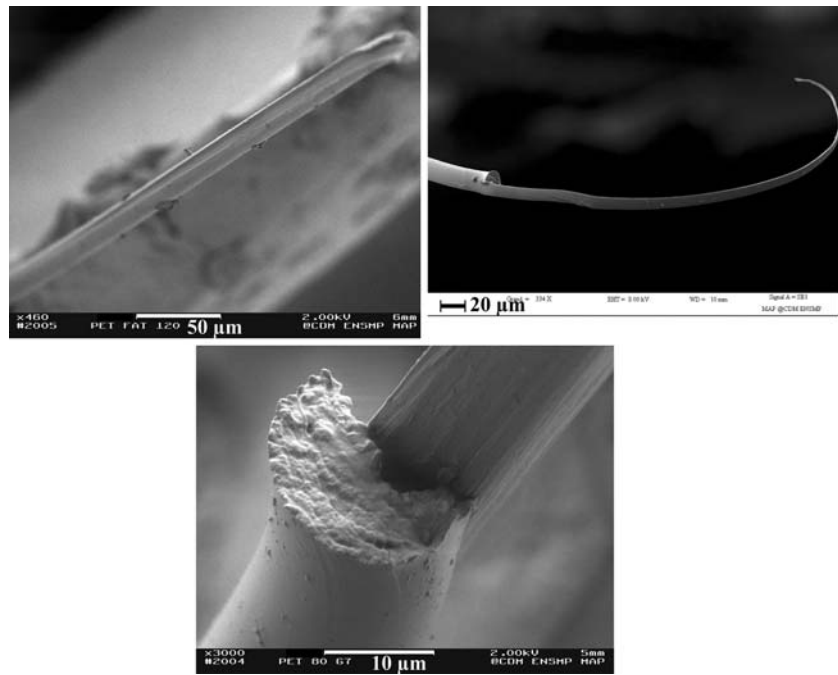
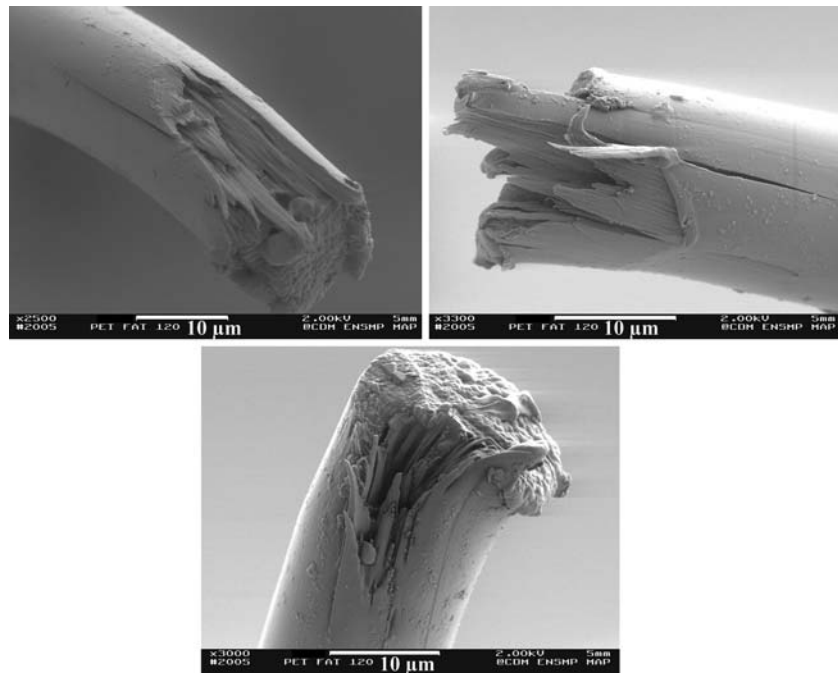


**Fig. 17** Fracture morphologies of fatigue tested fibres at 120 °C, presenting a truncated tongue and a complicated plastically deformed part



fail. These were extracted and observed with the SEM. As shown in Fig. 18, three types of fracture morphologies were clearly observed, corresponding to tensile or creep failure for 15% of the fibres, fatigue failure at room temperature for 20% and 65% to hot fatigue tests. As the tests were carried out at 20 °C it is clear that dissipative energy caused

by internal damping produced heating of the yarn. As a consequence of these observations, a thermocouple was placed in the middle of the yarn and the results are presented on Fig. 19. Studying different mechanical conditions, it appeared that the temperature rise was directly linked to the imposed load amplitude, as presented in Fig. 20. For similar load

**Fig. 18** Fractured morphologies of fibres extracted from fatigue tested yarn at ambient temperature, three different facies are observed traction or creep, fatigue at ambient temperature and mainly fatigue in hot conditions

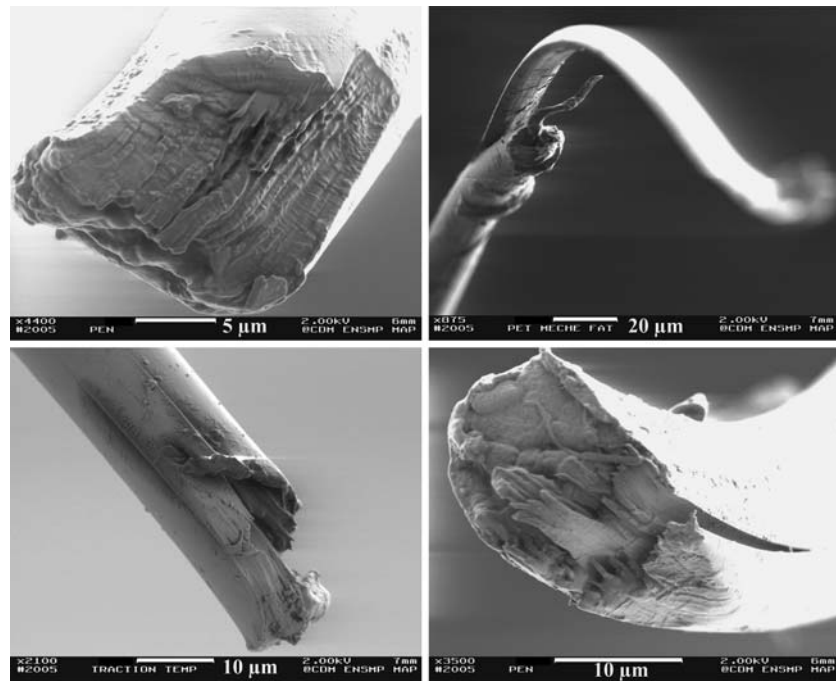
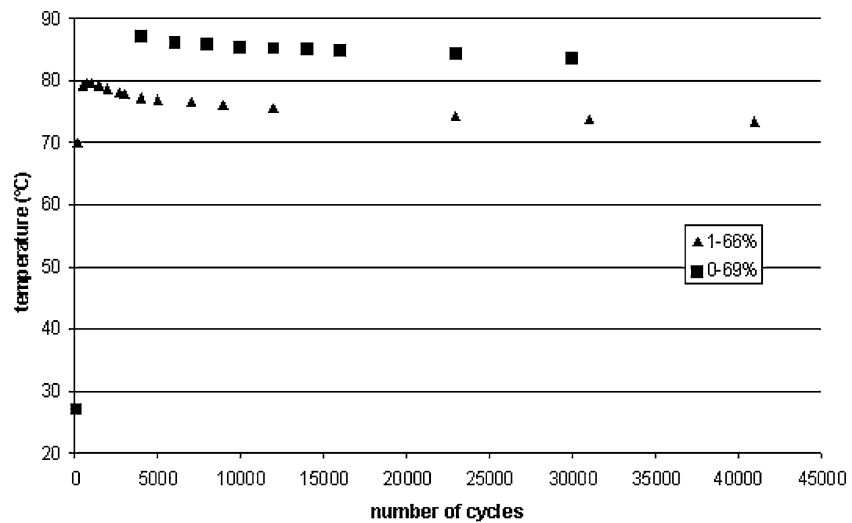


**Fig. 19** Example of temperature rise in a yarn during a fatigue test at 50 Hz for two different conditions: 1–66% of breaking load (round) and 0–70% of breaking load (square)



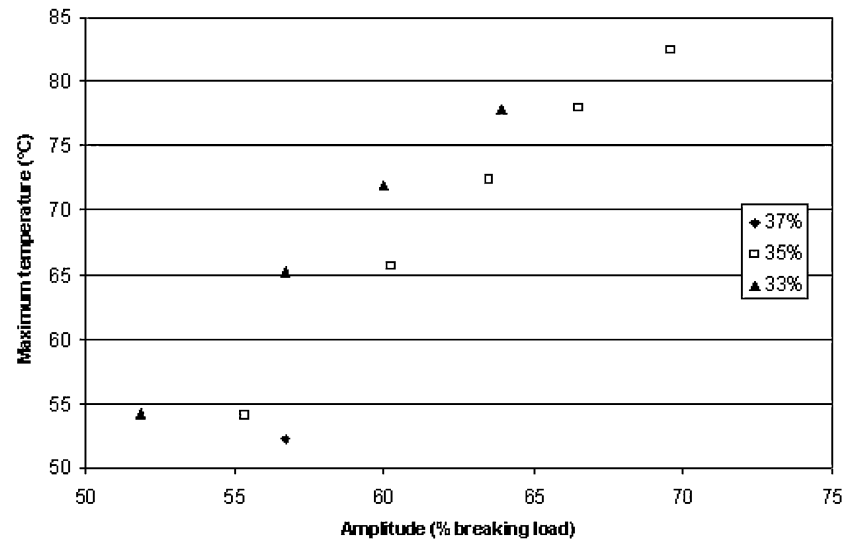
amplitudes, the smaller the mean load, the greater the rise in temperature. Multidyn software allowed the dissipative energy per cycle to be calculated.

**Discussion**

Oudet’s model of thermoplastic fibre structure [4] can be used to explain the different parts of the stress/strain curves presented in the results. During the first stage of deformation, Raman studies carried out by Marcellan [14, 15] showed that, in the case of nylon fibres, there was no change in the crystalline phase;

indeed, there was no participation of this phase in elongation. Thus, it is the intrafibrillar amorphous zones which accommodate the deformation due to three-dimensional geometrical movements and conformation changes in the molecular structure. The decrease of the slope and the general shape of this first region in the curve are similar to the extension of rubber but on a much smaller deformation scale: the amorphous zone is around 50–100 nm long as the crystallinity rate is around 50% and the long period is around 140 nm, and interfibrillar molecules block some movements. This hypothesis is supported by the results showing the influence of the temperature. Above the

**Fig. 20** Evolution of maximum temperature with the cycle amplitude for different mean load (31, 33 and 35% of the breaking load)



glass transition temperature, this region disappears, thermal fluctuations give sufficient energy to make the entire conformations equivalent and it becomes easier to deform the PET fibre. The result is that the initial modulus decreases. Finally, for small deformations, the deformation mechanism corresponds to rubber elasticity behaviour with respect to the small amorphous zone sizes and cross linking chains blocking extension.

The second region of deformation involves more energetic phenomena. Previous Raman studies highlight the main role of oriented and crystalline zones; chemical bonds extend and molecular angles open. The result is however that the temperature has less influence on the mechanical behaviour as the second modulus loses only 30% of its room temperature value when measured at 120 °C.

The plateau of the third region is due to a load threshold. To better understand the processes involved in this phase, another experiment was carried out. The fibre was loaded monotonically, past the second inflexion point, to 95% of the breaking load. Then, after total relaxation, the fibre was stretched until failure and during the second loading, the modulus was seen to be equal to its initial value. This clearly shows that there can be very little molecular breakage occurring as, in this case, the stiffness would fall during the second loading. The deformation in this third region must be due to irreversible sliding in the crystalline zones or between fibrils which does not become possible except if a load threshold level is exceeded and this threshold falls with increasing temperature. The threshold can therefore be seen as an energy threshold level beyond which sliding at the molecular level becomes possible. This part could be compared to

yielding in metal as the compliance changed and the irreversible character of this part.

The glass transition temperature was determined with three different techniques: DSC, DMTA and tensile tests on single fibres. These techniques gave values for  $T_g$  as 110, 111, 100 °C. The transition at the molecular level can be seen to occur over a temperature range, from 70 °C to 140 °C. The concordance between these values is noticeable because of the main differences between the experiments, as presented on Table 1. Increasing the temperature beyond the  $T_g$  has the effect of modifying a considerable number of parameters including initial modulus, calorific capacity and loss tangent. Intrinsic characteristics of the material evolve with temperature; the glass transition affects mainly the zone controlled by the amorphous phase i.e. at low strain. However, the variations of tensile and creep fracture morphologies suggest that plastic deformation is more likely to occur at and above the glass transition temperature.

Experimental results presented above show that temperature is an important parameter in determining the creep lifetimes of polyester fibres. In the 1970s, Zhurkov introduced an empirical relation [16] derived from the Arrhenius probabilistic approach, to calculate the failure probability of thermoplastics. It has been applied to numerous types of material and in particular to PET fibres [17]. The main premise is that loading raises the energy of the system, reducing energy barriers necessary for the breaking of atomic bonds. The accumulation of associated bond failures leads to the development of a microcrack; and, percolation of microcracks through the fibre finally causes failure. The Zhurkov formula gives the creep

**Table 1** Main differences between the different tests used to determine Glass temperature

	DSC	DMTA	Tensile test
Observed physical phenomena	Thermal	Thermomechanical	Thermomechanical
Characteristic Time of sollicitation	–	High (50 Hz)	Small (20 s)
Temperature conditions	10 °C/min	10 °C/min ± 2 °C each 80 s	Static temperature
Material quantities	5 mg	yarn (~400 fibres)	1 fibre
Parameters used for Tg determination	Heat flow	Young modulus Loss tangent	Young modulus

lifetime of a sample under a stress  $\sigma$  and at temperature  $T$  in Kelvin:

$$\tau = \tau_0 \exp\left(\frac{U - \gamma\sigma}{RT}\right)$$

In this formula,  $U$  corresponds to the energy threshold necessary to break the weakest bond of the polyester molecule,  $RT$  is the Boltzman factor expressing the thermal energy fluctuation,  $\tau_0$  is a period inverse of the testing frequency.  $\gamma$  is a structural factor expressing the equivalence between load and energy and includes the statistics of local overloading occurring.

A correlation between the median lifetimes observed and the formula permits the different values to be obtained:

$$\begin{aligned} \tau_0 &= 6.2 \times 10^{-14} \text{ si.e.f} = 540 \text{ cm}^{-1} \\ U &= 214 \text{ kJ/mol} \\ \gamma &= 140 \text{ kJ/mol/MPa} \end{aligned}$$

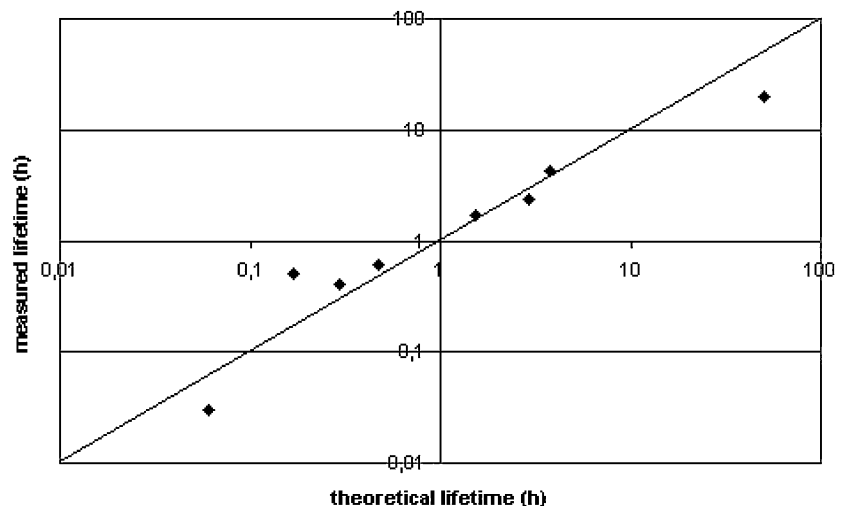
These numbers could be compared to typical physical ones: the vibration frequency of intermolecular bonds could be 630, 860, 1100, 1300  $\text{cm}^{-1}$ , as observed in Raman studies. The bond energy is 260 kJ/mol/MPa for the weakest. This approach allows theoretical

lifetimes for different load and thermal conditions to be predicted. Fig. 21 shows a comparison between experimental median lifetimes and those calculated using this formula.

The oscillating tests made on single fibres show that the minimum load is an as important criterion for fatigue failure as is the maximum load and confirms other studies which indicate that the minimum load must be below a threshold, as presented in Fig. 14. The median lifetime of a cyclic test 10–80% is four times the median lifetime of a 0–80% test even though the mean load is higher. This paradoxical behaviour is an important characteristic of the fatigue of fibres; it has been reported in other studies on single fibres [6, 7–9], Winkler [11] in a study on disk fatigue tests on PET yarns presented the retained strength of yarn for various deformation conditions : -5%/-20%, +5%/-10%, +10%/-5% and +20%/+5%. High tension with low compression gives the highest strength loss. Furthermore, fatigue experiments conducted on yarn make also clear the effect of the minimum load: for identical amplitude, the temperature increase is higher for lower minimum loads. It is around zero minimum load that the system dissipates greatest energy.

During fatigue, the main damage comes from the load bearing section being reduced by the penetration of the longitudinal crack into the fibre, which increases the real

**Fig. 21** Correlation between calculated and measured lifetime for the different conditions studied



applied stress and locally accelerates creep degradation. At high temperature, the creep phenomena is amplified and plastic deformation occurs more easily. Indeed, as soon as the longitudinal crack is created and removes a small section of the fibre from load bearing, the increased stress in the remaining section in the vicinity of the crack causes plastic deformation and then creep rupture without real longitudinal propagation. The result is that the complementary fracture morphologies are symmetrical, the three phase process of fatigue failure at room temperature with longitudinal crack initiation, propagation while section reduction and creep failure is replaced by a two phase process with longitudinal crack initiation but limited longitudinal crack growth and accelerated creep rupture. It explains the differences in fracture morphologies with a truncated tongue but also the reduction of lifetimes which is less important than for creep tests. Fatigue crack initiation is, in this case, the major part of fatigue life. This type of failure, with a truncated tongue, has been observed by Winkler [11] and Naskar [13] in failed yarns extracted from rubber after disk fatigue tests. With heat generation in rubber and in yarns, the temperature must be around the glass transition so that it is understandable that fracture morphologies typical of high temperature failure can be seen even if the yarn is nominally tested at room temperature. The studies on single fibres confirm that the origin of this type of failure morphology is due to extension fatigue.

During cyclic loading, the stress/strain curve shows a hysteresis loop the area within which corresponds to the mechanical energy dissipated. This mechanical energy follows a decreasing logarithmic law during the test and can be expressed as:

$$E_m = E_0 - A \ln(N) \quad \text{with} \quad \begin{cases} E_0 \text{ initial mechanical energy} \\ A \text{ log law coefficient} \\ N \text{ number of cycles} \end{cases}$$

The result is an increase in yarn temperature and follows a classical calorific law:

$$E_{\text{ext}} = -mC_p dT \quad \text{with} \quad \begin{cases} m \text{ material mass} \\ C_p \text{ calorific coefficient} \\ dT \text{ temperature variation} \\ \text{during a cycle.} \end{cases}$$

The whole system of heat exchange with the exterior with a thermal exchange coefficient  $h$  and via a surface  $S$ , is given by:

$$E_{\text{exc}} = -hS(T - T_{\infty}) \quad \text{with} \quad \begin{cases} T \text{ yarn temperature} \\ T_{\infty} \text{ air temperature} \end{cases}$$

The thermal parameters  $C_p$  and  $h$  are to be found in any polymer handbook together with heat and mass transfer data,  $h$  has a natural convection part and a radiation part following Stefan's law.

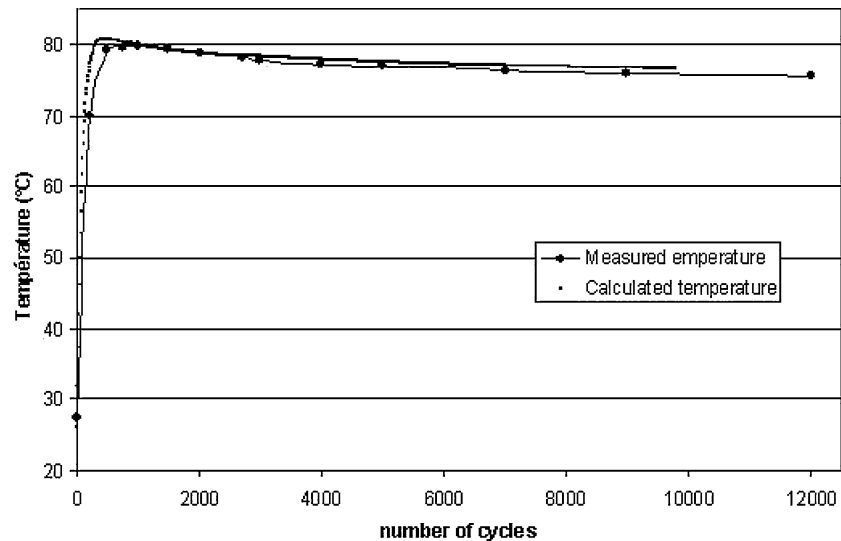
An iterative calculation allows the theoretical temperature versus the number of cycles to be obtained, as shown in Fig. 22. The result fits very well with the measured temperature. The temperature increase is directly linked to the mechanical dissipative energy i.e. the mechanical oscillation amplitude. A study on disk fatigue tests, done by Yabuki [12], links fatigue lifetime to the inverse of the temperature of the rubber tube containing yarns subjected to cyclic sollicitation. It considers that the temperature increase is due to rubber hysteresis, but the heat generation can also come from yarn.

In addition to heat generation, the mechanical cyclic loading induces the failure of the fibres in the yarn. At first, a few fibres which are more stretched than others support a greater part of the applied load and break through tensile elongation or rapid creep. Secondly, fibres at the periphery of the yarn and consequently less heated, develop fatigue cracks showing a tongue of material, as in the fatigue failure of single fibres at room temperature. In a third stage, most of the fibres fail and show truncated tongues, characteristic of fatigue damage at raised temperatures. It is clear that load cycling of a yarn provokes the fatigue process and the initial damage is due to the classical fatigue process as observed at room temperature on single fibres but also due to the fatigue process at raised temperatures. Finally, when a few percent of the fibres are broken, the overload on the whole yarn causes creep and tensile failure of fibres and the failure of the complete yarn.

## Conclusion

The transition from a glassy to a rubbery state as temperature increases, has a great influence on the first part of the stress/strain curve of PET fibres as it concerns low energetic conformation changes. The increase in temperature lowers the breaking load. Creep damage is accelerated as temperature increases. The creep phenomena can be described well with the Zhurkov model; it allows lifetimes for different temperatures and load conditions to be predicted. Cyclic mechanical loading of a single fibre can provoke

**Fig. 22** Theoretical approach of the heat generation and dissipation during a fatigue test on yarn with  $E_0 = 7$  mJ/cycle,  $S = 2.5 \cdot 10^{-4}$  m<sup>2</sup>,  $m = 4$  mg,  $T = 0.02$  s and  $A = 0.15$ J



fatigue failure before failure occurs by the creep mechanism. In order to fail in fatigue, certain conditions have to be present such as minimum load levels, load amplitudes and failure leads to distinctive fracture morphologies. Above 80 °C, these phenomena remain more damaging than creep but the fracture morphologies of the broken fibres are slightly modified and show a very specific truncated tongue. Finally, it has been seen that the results on single fibres give good clues to yarn mechanical behaviour. Thus, the modulus variation with respect to the glass transition temperature and the fatigue phenomena observed with single fibres are indicative of behaviour of the complete yarn.

**Acknowledgements** The authors wish to thank B. Monasse for help with the discussion and Y. Favry for his technical assistance.

## References

1. Lin YJ, Hwang SJ (2004) *Math Comput Simul* 67:235
2. Jeon HY, Cho SH, Mok MS, Park YM, Jang JW (2005) *Polym test* 24:339
3. Prevorsek DC, Harget PJ, Sharma RK (1973) *J Macromol Sci B* 8:127
4. Oudet C, Contribution à l'Etude de l'endommagement par fatigue des fibres de polyester à usage technique, Ph.D. thesis, ENSMP, 1986
5. Bunsell AR, Hearle JWS (1974) *J Appl Polym Sci* 18:267
6. Oudet C, Bunsell AR, Hagege R, Sotton M (1984) *J Appl Polym Sci* 29:363
7. Lechat C, Bunsell AR (2006) *J Mater Sci* 41(6):1745
8. Herrera Ramirez J, « Les mécanismes de fatigue dans les fibres thermoplastiques », PhD thesis, ENSMP, 2004
9. Herrera Ramirez J, Bunsell AR (2005) *J Mater Sci Lett* 40:1269
10. Bunsell AR, Hearle JWS, Hunter RD (1971) *J Phys E: Scientific Instrument* 4:868
11. Winkler EM (1991) *Textile Res J* 61(8):441
12. Yabuki K, Iwasaki M, Aoki Y (1986) *Text Research institute* 56(1):43
13. Naskar AK, Mukherjee AK (2004) *Polym Degrad Stabil* 83(1):173
14. Marcellan A, Microstructures, Micromécanismes et comportement à rupture des fibres de PA66. PhD thesis, ENSMP, 2003
15. Marcellan A, Colombari P, Bunsell AR (2004) *J Raman Spectrosc* 35:308
16. Zhurkov SN, Zakrevskiy VA, Korsukov VE, Kuksenko VE (1972) *J Polym Sci* 10(A-2):1509
17. Zeifman MI, Ingman D (2000) *J Appl Phys* 88(1):76